

Article

Midge Paleo-Communities (Diptera Chironomidae) as Indicators of Flood Regime Variations in a High-Mountain Lake (Italian Western Alps): Implications for Global Change

Marco Bertoli ¹, Gianguido Salvi ^{2,3}, Rachele Morsanuto ¹, Elena Pavoni ², Paolo Pastorino ^{4,*}, Giuseppe Esposito ⁴, Damia Barceló ⁵, Marino Prearo ⁴ and Elisabetta Pizzul ¹

- ¹ Dipartimento di Scienze della Vita, Università degli Studi di Trieste, Via Giorgieri 10, 34127 Trieste, Italy; marco.ber3@gmail.com (M.B.); rachele.morsanuto@studenti.units.it (R.M.); pizzul@units.it (E.P.)
- ² Dipartimento di Matematica, Informatica e Geoscienze (MIGe), Università degli Studi di Trieste, Via Weiss 2, 34128 Trieste, Italy; gsalvi@units.it (G.S.); epavoni@units.it (E.P.)
- ³ Consiglio Nazionale delle Ricerche, Istituto di Scienze Polari (CNR-ISP), Via Torino 155, 30172 Mestre, Italy
- ⁴ Istituto Zooprofilattico del Piemonte, Liguria e Valle d'Aosta, Via Bologna 148, 10154 Torino, Italy; giuseppe.esposito@izsto.it (G.E.); marino.prearo@izsto.it (M.P.)
- ⁵ Chemistry and Physics Department, University of Almeria, Ctra Sacramento s/n, 04120 Almería, Spain; damiab@ual.es
- * Correspondence: paolo.pastorino@izsto.it; Tel.: +39-0112686251

Abstract: Sediments of alpine lakes serve as crucial records that reveal the history of lacustrine basins, offering valuable insights into the effects of global changes. One significant effect is the variation in rainfall regimes, which can substantially influence nutrient loads and sedimentation rates in lacustrine ecosystems, thereby playing a pivotal role in shaping biotic communities. In this study, we analyze subfossil chironomid assemblages within a sediment core from an alpine lake (western Italian Alps) to investigate the effects of rainfall and flood regime variations over the past 1200 years. Sediment characterization results highlight changes in sediment textures and C/N ratio values, indicating phases of major material influx from the surrounding landscape into the lake basin. These influxes are likely associated with intense flooding events linked to heavy rainfall periods over time. Flooding events are reflected in changes in chironomid assemblages, which in our samples are primarily related to variations in sediment texture and nutrient loads from the surrounding landscape. Increased abundances of certain taxa (i.e., *Brillia*, *Chaetocladius*, *Cricotopus*, *Psectrocladius*, *Cricotopus/Orthocladius Parorthocladius*) may be linked to higher organic matter and vegetation inputs from the surrounding landscape. Biodiversity decreased during certain periods along the core profile due to intense flood regimes and extreme events. These results contribute to our understanding of alpine lake system dynamics, particularly those associated with intense flooding events, which are still understudied.

Keywords: chironomidae assemblages; environmental features; flood regimes; paleolimnology



Citation: Bertoli, M.; Salvi, G.; Morsanuto, R.; Pavoni, E.; Pastorino, P.; Esposito, G.; Barceló, D.; Prearo, M.; Pizzul, E. Midge Paleo-Communities (Diptera Chironomidae) as Indicators of Flood Regime Variations in a High-Mountain Lake (Italian Western Alps): Implications for Global Change. *Diversity* **2024**, *16*, 693. <https://doi.org/10.3390/d16110693>

Academic Editors: Michael Wink and Vassiliki Kati

Received: 6 October 2024

Revised: 4 November 2024

Accepted: 5 November 2024

Published: 12 November 2024



Copyright: © 2024 by the authors. Licensee MDPI, Basel, Switzerland. This article is an open access article distributed under the terms and conditions of the Creative Commons Attribution (CC BY) license (<https://creativecommons.org/licenses/by/4.0/>).

1. Introduction

Alpine lakes are often considered key indicators of environmental health due to their sensitivity to human activities and their typically untouched nature, a result of their remote, sparsely populated locations. Despite their pristine appearance, these ecosystems undergo changes in their physical, chemical, biological, and morphological properties [1,2]. They are influenced by local activities such as water extraction, tourism, and the introduction of alien species, as well as global factors like long-distance pollution, acid rain, and climate change [3,4]. These lakes, commonly found in mountainous areas, capture erosion materials from their surroundings, and their sediments provide important historical environmental data. They are also valuable for studying ecological changes, particularly those related to global warming [5,6]. Mountain regions are particularly vulnerable to climate change, as

demonstrated by the disparity between high-elevation mean temperatures and global averages [7,8]. Increased greenhouse gas levels have led to more frequent heavy precipitation events due to changes in atmospheric moisture transport [9]. These areas frequently experience severe floods, which cause notable damage, and variations in rainfall patterns can notably influence nutrient and sedimentation levels in lakes. By identifying sediment layers in different energy environments, researchers can reconstruct past alluvial phases linked to climatic trends and heavy rainfall events [10,11]. The thickness of these deposits can also indicate the intensity of such events [12,13]. While studying alpine lake sediment records can yield valuable insights, interpreting these records within the context of climate change is challenging [8]. The impact of global warming on flood activity in mountainous regions is notable, with an increase in extreme precipitation events observed in the European Alps since the 1980s [7,8,14]. These changes also affect biotic communities, including those used as environmental indicators and paleolimnological proxies. Chironomid assemblages, whose larval head capsules are well-preserved in lake sediments, are crucial biological proxies [15–17]. They are influenced by water temperature [15,18,19] and other factors such as trophic conditions and sediment characteristics [20]. The introduction of fish can alter chironomid communities, as shown in recent paleolimnological research [6,17].

This study focuses on subfossil chironomid assemblages in Upper Balma Lake, located in the western Italian Alps (Piedmont, Italy), a site not previously studied from a paleolimnological standpoint. The main goals were to examine the relationship between changes in chironomid communities and variations in rainfall and flood patterns by (i) analyzing lake sediments for grain size and geochemical properties, (ii) identifying subfossil chironomid assemblages, and (iii) exploring the connections between biotic assemblages and changes in trophic conditions and sediment geochemistry in relation to rainfall and flood regime changes. We hypothesize that changes in rainfall and flood patterns would have influenced chironomid communities over time, both directly through extreme events and indirectly by modifying nutrient loads and sediment characteristics. The presence of fish was also considered, as it could affect data interpretation, particularly in historically fishless alpine lakes where non-native species were introduced for fishing purposes in the late 20th century [2].

2. Materials and Methods

2.1. Study Area

The research was conducted at Upper Balma Lake, a typical alpine lentic environment in the Cottian Alps, situated within the Municipality of Coazze (Piedmont, Northwest Italy) at an elevation of 2216 m above sea level (a.s.l.) (Figure 1a). This glacial lake has an S-shaped basin divided into two sub-basins by a shallow mid-section. Its perimeter is 774 m, surface area 1.82 ha, and maximum depth 2.77 m. The catchment area is primarily ophiolite metamorphic bedrock. There is a small grassy area situated to the south where a small stream enters, while another stream begins at the northeast corner and flows into the Lower Lake. These lakes constitute a two-lake alpine system that has been examined in previous ecological and ecotoxicological studies, i.e., [21,22].

Both lakes are situated within the Special Area of Conservation (SAC) and Special Protection Area (SPA) IT1110006 “Orsiera Rocciavère” and are part of the Orsiera Rocciavère Natural Park.

During the latter part of the 20th century, the primary influences on the region included the distant transport of pollutants from urban areas, grazing, and fishing activities [21]. Originally devoid of fish, brook trout (*Salvelinus fontinalis* Mitchell, 1814) were introduced for recreational angling in the 1970s [21,22]. Key physicochemical (temperature, dissolved oxygen, pH, conductivity, and alkalinity) and nutrient (ammonia, nitrate, and phosphorus) water parameters were assessed on-site using field probe (Hanna Instruments Inc. model HI98494-multiparameter, Woonsocket, RI, USA) and documented throughout 2021, as detailed in Table 1.

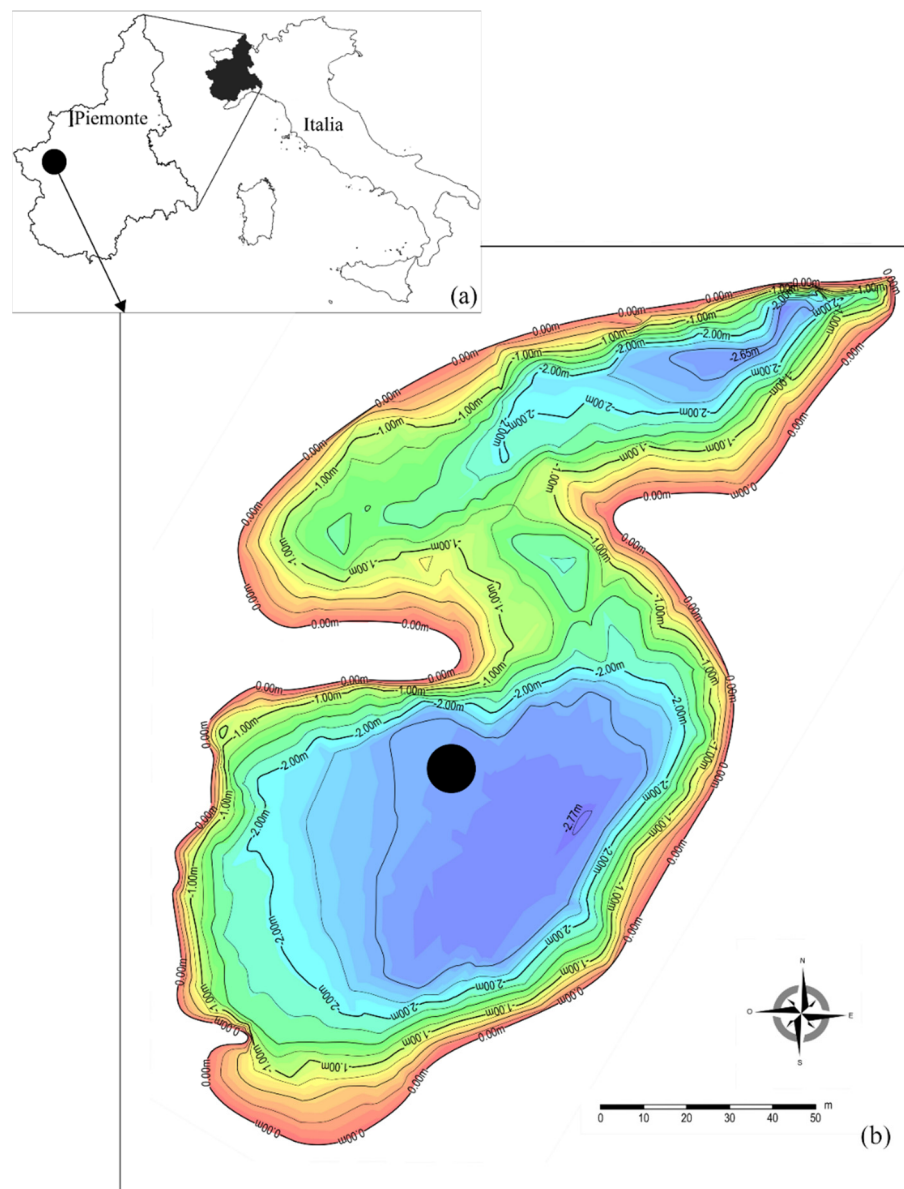


Figure 1. (a) Study area and (b) location of the sampling site in Upper Balma Lake.

Table 1. The mean values and standard deviations (S.D.) of the water physicochemical parameters measured at Upper Balma Lake.

Parameter	Mean		S.D.
Temperature (°C)	8.61	±	2.94
Dissolved oxygen concentration (mg L ⁻¹)	6.50	±	0.33
pH (unit)	7.40	±	0.19
Conductivity (µS cm ⁻¹)	12.81	±	1.35
Alkalinity (mg/L)	47.31	±	16.60
Secchi Disk (m)	1.1	±	0.1
NH ₄ ⁺ (mg L ⁻¹)	0.04	±	0.02
NO ₃ ⁻ (mg L ⁻¹)	2.75	±	1.47
P (mg L ⁻¹)	0.05	±	0.02

2.2. Core Sampling and Sediment Characterization

In July 2021, a coring campaign was carried out using a 50 mm gravity Kajak-type sediment corer [15]. A single 40 cm long core was retrieved from a deep section of the lake

(Figure 1), sealed in a sampling tube, and stored at $-20\text{ }^{\circ}\text{C}$. The core was then sectioned into 37 transverse slices, each approximately 1 cm thick, based on guidelines for paleolimnological studies in mountain lakes [15,22,23]. Each section was further divided into two sub-sections to analyze core chemistry, trace element concentrations, and grain size. The sections were labeled with “L” followed by a number from “1” to “37” (L1 representing the top section and L37 the bottom), then frozen at $-20\text{ }^{\circ}\text{C}$. Subsequently, the samples were freeze-dried through vacuum evaporation. For textural analysis, each section was filtered using a $1000\text{ }\mu\text{m}$ mesh size filter. The residues were set aside while the remaining sediments were analyzed with a Malvern Mastersizer 3000 laser diffraction particle size analyzer, Worcestershire, UK. The one percentile coarse granule (C_{μ}) and the median diameter (M_{μ}) in micrometers were used as indices of high transport capacity.

2.3. Core Chemistry (Organic Matter, C/N Ratio and Trace Elements Analyses) and Core Dating

Three separate aliquots, each comprising about 10–20 μg , were extracted from each section for the analysis of total carbon (C_{tot}), total organic carbon (TOC%), and total nitrogen (TN%). The samples were pulverized using an agate mill and dried in an oven at $105\text{ }^{\circ}\text{C}$ for 24 h. Total Organic Carbon (TOC) analysis involved acidifying the samples with HCl, gradually increasing its concentration to 18%. Determination of TOC and TN was performed using a CHN Analyzer (ECS 4010 CHNSO; Costech Analytical Technologies Inc., Valencia, CA, USA) [24], followed by calculation of the C/N ratio.

For trace element (Pb, Mn, Zn, As, Mo, and Cd) analysis, freeze-dried sediment samples (CoolSafe 55-4 SCANVAC) were manually ground using an agate mill. Aliquots of 0.250 g underwent acid digestion in PTFE vessels within a closed microwave system (Multiwave PRO, Anton Paar, Graz, Austria). The digestion process included a certified reference material (PACS-3 Marine Sediment Certified Reference Material, NRCC, Whitehorse, YT, Canada) to ensure accuracy, achieving recoveries between 88% and 107%. Acid digestion was carried out with a mixture of 5 mL nitric acid (HNO_3 , 67–69%), 1 mL hydrochloric acid (HCl, 34–37%), 1 mL hydrofluoric acid (HF, 48%), 4 mL boric acid (H_3BO_3 , 6%), and 0.5 mL hydrogen peroxide (H_2O_2 , 30%), following a modified EPA Method 3052. The mineralization process involved two heating steps and H_3BO_3 was added during the second step to neutralize excess HF. The resulting solutions were diluted to 25 mL with MilliQ water, further diluted 1:20, and analyzed via ICP-MS using a NexION 350X Spectrometer with an ESI SC Autosampler (PerkinElmer, Waltham, MA, USA). The instrument calibration utilized five standard solutions (0.5 to $100\text{ }\mu\text{g L}^{-1}$) prepared by diluting a multistandard solution for ICP analysis (10 mg L^{-1} , Periodic Table MIX 1 and MIX2, Sigma Aldrich Milan, Italy). The analytical precision, expressed as RSD%, was less than 3%.

Two bulk sediment samples, obtained from depths of 17–37 cm, were freeze-dried for AMS (Accelerator Mass Spectrometry) radiocarbon dating. Radiocarbon ages were determined at the Poznan Radiocarbon Laboratory (Poznan, Poland), employing the calibration dataset by Heaton et al. [25]. Lead (Pb) pollution data were incorporated to establish an age-depth model [6,8,25–33]. The age-depth model for Upper Balma Lake was constructed using the RStudio Package rbacon, updated to version 3.10 [34]. This approach employs Bayesian statistics to reconstruct accumulation histories by integrating radiocarbon and other dating outcomes. The modeling yielded four distinct age groups for further examination.

2.4. Chironomid Head Capsule Identification

The extraction of head capsules (HCs) followed the protocols described by Brooks et al. [15]. Initially, the samples were dispersed in warm distilled water ($40\text{ }^{\circ}\text{C}$) for 20 min and then filtered through a $100\text{ }\mu\text{m}$ mesh. The remaining residues were carefully examined, and chironomid HCs were isolated using a stereomicroscope with a minimum magnification of $25\times$. To ensure robust statistical outcomes, each sample was processed to yield a minimum of 100 HCs per section [6,15]. Subsequently, the HCs underwent gradual dehy-

dration in 80% and 100% ethanol (5 min per step) before being mounted on microscope slides with the ventral side facing up using Euparal[®] essence.

Identification of the HCs to the genus or species level (where feasible) was conducted using an optical microscope set at 60×–100× magnification, following identification references such as Oliver [35], Pinder and Reiss [36], Sæther [37], Brooks et al. [15], Lencioni et al. [38], Moller Pillot [11,39,40], and Andersen et al. [4]. For each core section, three subsamples were analyzed for statistical validity, with each subsample containing more than the recommended minimum of 50 HCs ($n > 50$), as advised by Brooks et al. [15].

2.5. Statistical Analyses

To examine changes in chironomid communities over the core's depth, taxa appearing in at least two samples with percentages exceeding 2% were included. Prior to analysis, data underwent log-transformation ($\log(x + 1)$) to mitigate the influence of highly abundant taxa [41]. A resemblance matrix was generated using the Bray–Curtis measure. Stratigraphic zones were identified using hierarchical cluster analysis with CONISS methodology, and cluster significance was assessed using the broken stick method [42–44], implemented via the rioja package in RStudio [45].

Differences among stratigraphic zones were evaluated using a one-way ANOSIM [46] with 999 permutations, due to significant results from the PERMDISP procedure [47]. The SIMPER test [46] identified key taxa contributing to the observed variability.

Redundancy Analysis (RDA) [48,49] was employed to examine relationships between biotic data and abiotic features across core sections. Redundancy Analysis was chosen based on Detrended Correspondence Analysis (DCA) indicating gradient lengths of less than 4 standard deviations [50]. To mitigate multicollinearity, a subset of variables was selected using Pearson correlation analyses. Variables with strong correlations ($r < |0.7|$, $p < 0.001$) were adjusted by excluding one of the correlated variables [51], with fish presence also included as a variable.

Variation partitioning analysis (VPA) [52] was then used to apportion the total explained variance among four variable groups: nutrients, trace elements, sediment characteristics, and fish presence. The contribution of each group was visualized using a Venn diagram. The significance and interactions of variable groups were assessed using Monte Carlo permutation tests (999 permutations). All analyses were performed in RStudio (version 2021.9.0.351) [53,54], with a significance level set at $p < 0.05$. Figures were created in RStudio and finalized using Inkscape (version 0.92).

3. Results

3.1. Core Geochemistry and Age-Depth Model

Sediment analysis allowed us to identify two main sections along the Upper Balma Lake core, corresponding to different depositional phases. From the bottom to the L13 section, sediment showed an alternation of coarse material and fine sediments. This alternation disappeared from the L12 section to the top of the core where specific sediment structures were not observed. This difference along the sediment core indicates a change in the sedimentation dynamic of the lake catchment. According to the Nota Classification, the Upper Balma core sediments were mainly represented by very sandy pelite and pelitic sand. Silt percentages were higher than clay and sands in 29 sections, while the remaining 8 samples showed higher levels of sand. Four sand peaks were identified in the core (L10, L19, L22, and L31) with the maximum value (88.6%) observed at L19 (Figure 2). Values of C_{μ} ranged between 1855 μm (L22) and 395 μm (L30), whereas M_{μ} ranged between 413 μm (L22) and 35 μm (L34).

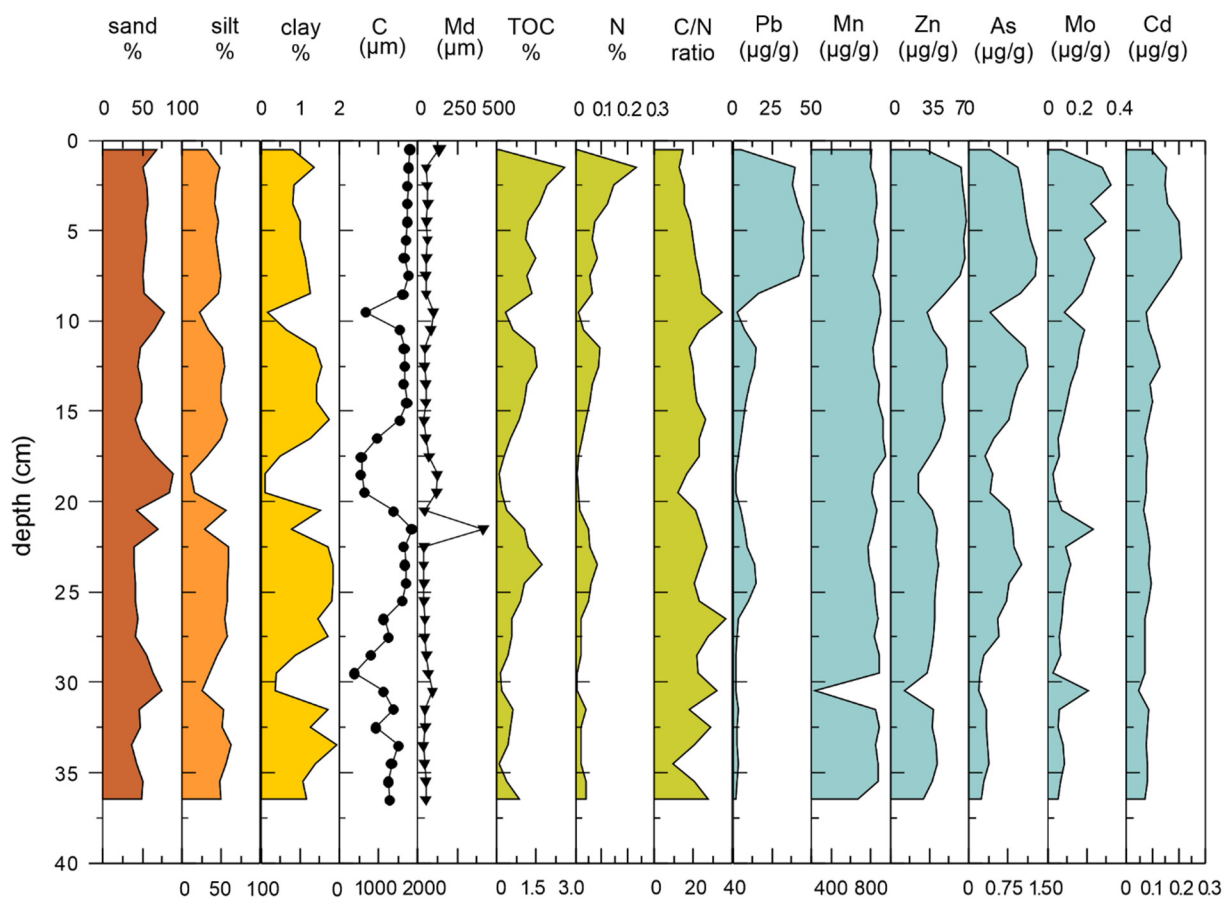


Figure 2. Stratigraphic diagram of the sedimentological and geochemical parameters measured in core sections sampled in the Upper Balma Lake. Results of the element analysis in light blue color are also reported.

Total Organic Carbon (TOC%) ranged between 0.07% (L1) and 2.65% (L2), whereas TN was between 0.005% (L18.5) and 0.23% (L1.5), showing parallel trends along the sediment core, with elevated percentages at the top of the core followed by intermediate peaks (L12 and L13 for TN and TOC, respectively, and L24 and L32 for both) alternated with decreasing values at L10, L19, and L30 (Figure 2). The C/N ratio reached the maximum value (36.4) at L27, whereas the minimum value (9.9) was observed at L35. Values generally exceeded 15, whereas peaks higher than 30 were observed at sections L10, L27, and L31. From the top to the bottom of the core, the trend showed an increasing phase, especially between sections L5 and L10, followed by a heavy decrease (sections L11–L12). Other significant decreasing points were recorded between L19–L20 and at L35 (Figure 2).

Regarding the trace elements, concentrations of Pb, Zn, As, Cd, and Mo showed a similar trend along the sediment core, with the highest values observed in the upper core sections (L1–L10) decreasing at the bottom (L20–L37) (Figure 2). In particular, the highest value for Pb ($45.1 \mu\text{g g}^{-1}$) was recorded at section L5, whereas the lowest was observed at section L30 ($1.6 \mu\text{g g}^{-1}$) (Figure 2). Intermediate peaks were found at sections L12 and L25 (slightly below $15 \mu\text{g g}^{-1}$). Similarly, Zn showed the maximum concentration at section L5 ($67.8 \mu\text{g g}^{-1}$), whereas the minimum value was recorded at section L31 ($12.5 \mu\text{g g}^{-1}$); in the case of As and Cd, the maximum peak was observed at section L7 ($1.3 \mu\text{g g}^{-1}$ and $0.2 \mu\text{g g}^{-1}$, respectively) and minimum at level L31 ($0.2 \mu\text{g g}^{-1}$ and $0.05 \mu\text{g g}^{-1}$, respectively). Concentrations of Cd were higher in levels L1–L13 and slightly constant in the lower sections. Values observed for Mo showed high variability, with several peaks along the core, maximum levels were observed at section L3 ($0.3 \mu\text{g g}^{-1}$) and minimum at L31 ($0.03 \mu\text{g g}^{-1}$). Finally, concentrations of Mn showed a constant trend with

increasing depth, ranging between $776 \mu\text{g g}^{-1}$ and $959 \mu\text{g g}^{-1}$, with the only exception represented by L31, which displays a lower concentration ($237 \mu\text{g g}^{-1}$).

The results of the radiocarbon analysis allowed us to date sections L19 and L33 (Table 2).

Table 2. Radiocarbon ages for samples of the Upper Balma Lake core.

Depth of Sample	Lab Code	^{14}C Age (Years BP)	Calibrated 2σ Age (Year BP)
18–19	BLM1 Poz-157773	920 ± 30	814–930
21–33	BLM3 Poz-158593	1155 ± 30	1097–1213

The Pb concentration ensured the indirect dating of surface levels (depth range: 0–10 cm) by recording the peak of Pb concentration dated at ca. 1970s, and then the decrease in concentration up to the present day. The obtained data and the information derived from the total Pb pollution analysis allowed us to build the age-depth model reported in Figure 3. The sedimentation rate calculated from the model was equal to $0.029 \text{ cm year}^{-1}$.

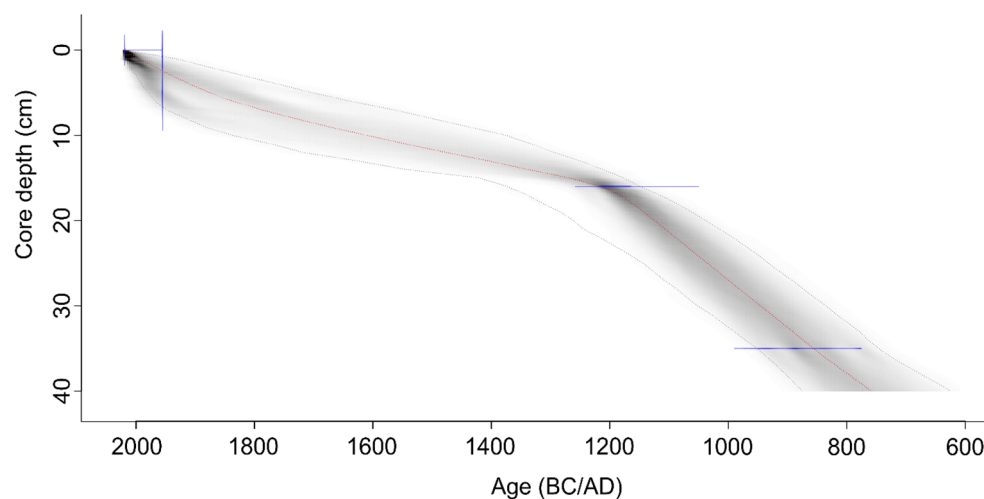


Figure 3. Bayesian age-depth model calculated for the Upper Balma Lake, based on 4000 interactions Markov Chain Monte Carlo. The dark gray areas represent the more precise dates, those in light gray the less precise dates; the red line indicates the best estimate of age for each level, and the black dashed lines the 95% confidence intervals.

3.2. Subfossil Chironomid Assemblages

The examination of the Upper Balma Lake core sample enabled the detection of 5413 chironomid head capsules (HCs) across 5 subfamilies and 25 genera. Consistent with Brooks et al. (2007), the abundance of HCs was notably substantial across all sections, consistently surpassing the threshold considered necessary for significant findings ($n > 50$), except for section L19, which yielded only a single capsule. The greatest concentration of HCs ($n = 436$) was recorded in section L5. Among the core sections, mean HC density was equal to $24.8 \pm 19.2 \text{ HC g}^{-1}$. Biodiversity showed fluctuating trends all along the core: total number of chironomid taxa ranged between 1 (L19) and 13 (L1, corresponding to the actual communities), while values of the Shannon–Wiener index ranged between 0 and 2.10, following the trend described for the number of observed taxa; on the other hand, dominance showed an opposite trend (Figure 4). Five periods of heavy reduction in biodiversity levels were highlighted at sections L2, L11, L19, L30, and L34, especially for section L19, where only *Paratanytarsus* was found, with few individuals in each sample. Subfamily Chironomidae was the most abundant along the core profile, especially the Tanytarsini tribe. Among them, genus *Paratanytarsus* was observed in all the sections with

high percentages (36.6–100%), whereas species *Corynocera oliveri* and genus *Micropsectra* were observed in almost all the core sections, ranging between 19.2–34.3% and 4.2–24.2%, respectively. Genus *Microtendipes* (tribe Chironomini) was recorded only in the top section L1. Subfamily Orthoclaadiinae showed the highest number of taxa along the core ($n = 21$). Among them, *Heterotrissocladius marcidus* was recorded in 20 sections, despite frequencies being generally low (0.35–4.4%). *Psectrocladius sordidellus* (0.23–4.11%) and the genus *Chaetocladius* (0.27–3.85%) were observed in 12 and 11 sections, respectively. The genera *Cricotopus* and *Hydrobaenus* were recovered in a few samples, but their frequencies were generally higher than previously observed Orthoclaadiinae (0.40–20.0% for *Cricotopus* and 1.61–7.0% for *Hydrobaenus*).

Four genera belonging to the subfamily Tanyptodinae were observed. *Macropelopia* was widely present (28 sections), with percentages ranging between 0.4 and 20.0%. Moreover, genus *Apsectrotanypus* (0.23–1.61%) was observed in 12 sections. Finally, genera *Zavrelimyia* (0.41–6.25%) and *Procladius* (0.35–1.45%) were found in 6 sections (Figure 4).

The cluster analysis based on the chironomid data allowed us to highlight stratigraphic zones or section groups, indicated with letters A–F from the top to the bottom of the core (Figures 4 and 5a). The significant number of groups was six, in agreement with the broken stick analysis (Figure 5b).

All these groups were significantly different from each other in terms of the composition of chironomid assemblages (ANOSIM $R = 0.361$, $p < 0.001$), except for group B (sections L5–L11), which was not different from groups C (sections L12–L16) and E (sections L22–L27). In this context, the SIMPER test highlighted that the main contribution to the observed variability was due to *Paratanytarsus*, *Corynocera oliveri*, *Micropsectra*, *Macropelopia*, and *Heterotrissocladius marcidus*, which were associated with 78.1% of the observed dissimilarity. The remaining taxa showed contributions lower than 3%, but they were still significant (Table 3).

Table 3. SIMPER test outcomes concerning chironomid communities noted in the sediment core of Upper Balma Lake for the sample groups identified through hierarchical cluster analysis.

Taxon	Av. Dissim.	Contrib. %	Cumulative %
<i>Paratanytarsus</i>	7.35	30.88	30.88
<i>Corynocera oliveri</i>	6.02	25.29	56.17
<i>Micropsectra</i>	3.76	15.8	71.97
<i>Macropelopia</i>	1.45	6.09	78.05
<i>Heterotrissocladius marcidus</i>	0.76	3.19	81.24
<i>Chaetocladius</i>	0.54	2.26	83.5
<i>Apsectrotanypus</i>	0.48	2.01	85.52
<i>Zavrelimyia</i>	0.46	1.93	87.45
<i>Psectrocladius sordidellus</i>	0.45	1.87	89.32
<i>Prodiamesa olivacea</i>	0.42	1.77	91.09
<i>Psectrocladius</i>	0.42	1.75	92.84
<i>Cricotopus</i>	0.41	1.74	94.58
<i>Hydrobaenus</i>	0.28	1.17	95.75

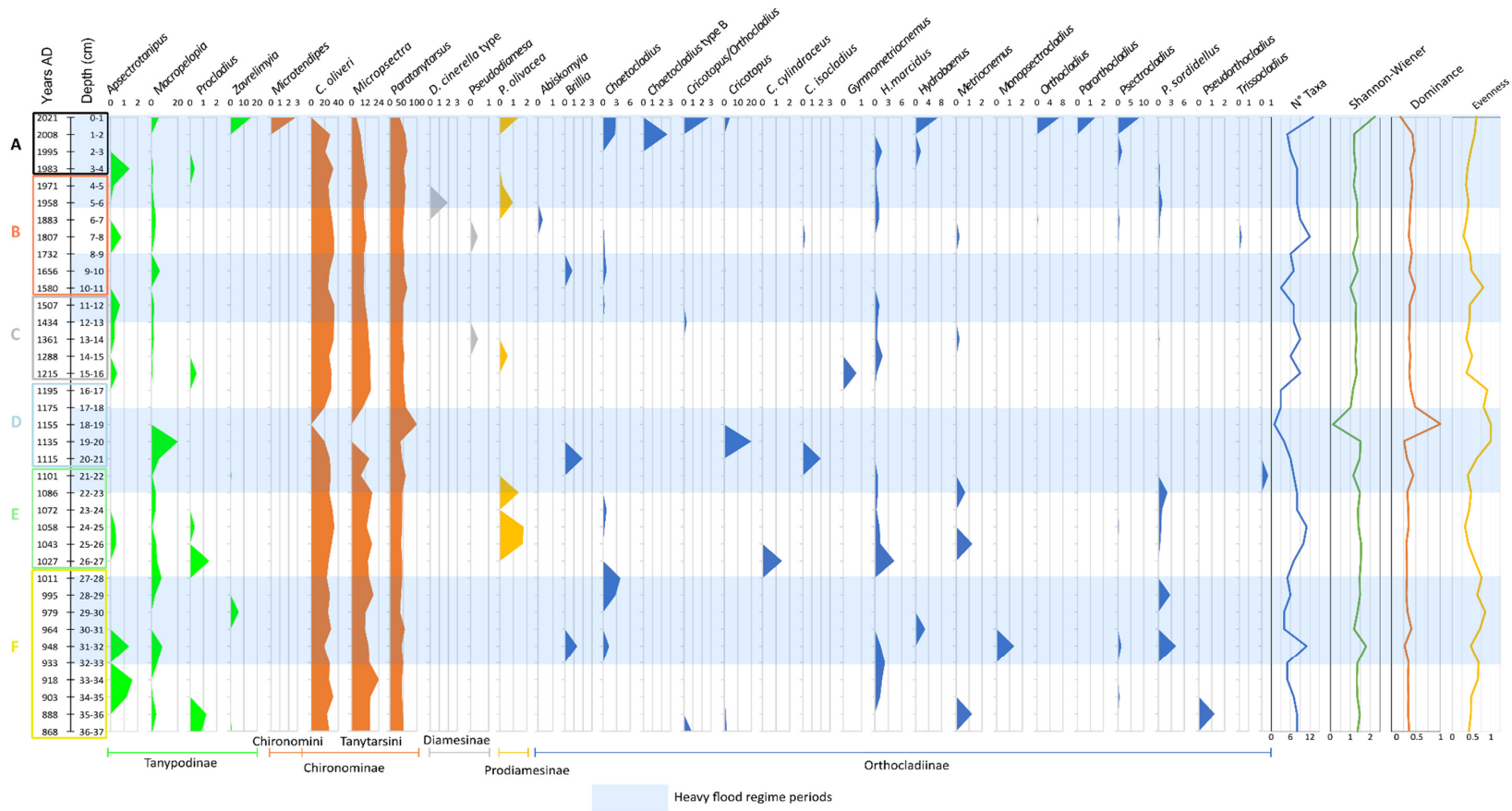


Figure 4. Relative abundances of the chironomid taxa observed in the Upper Balma Lake core sections and trends of the main community indices calculated along the core. Time periods with high flood regimes are indicated by the light blue bands superimposed on the graphs; identification of these periods is based on Giguet-Covex et al. [8] and Wilhelm et al. [55]. Group colors highlighted by cluster analysis and used in the RDA are reported (see Figures 5 and 6a).

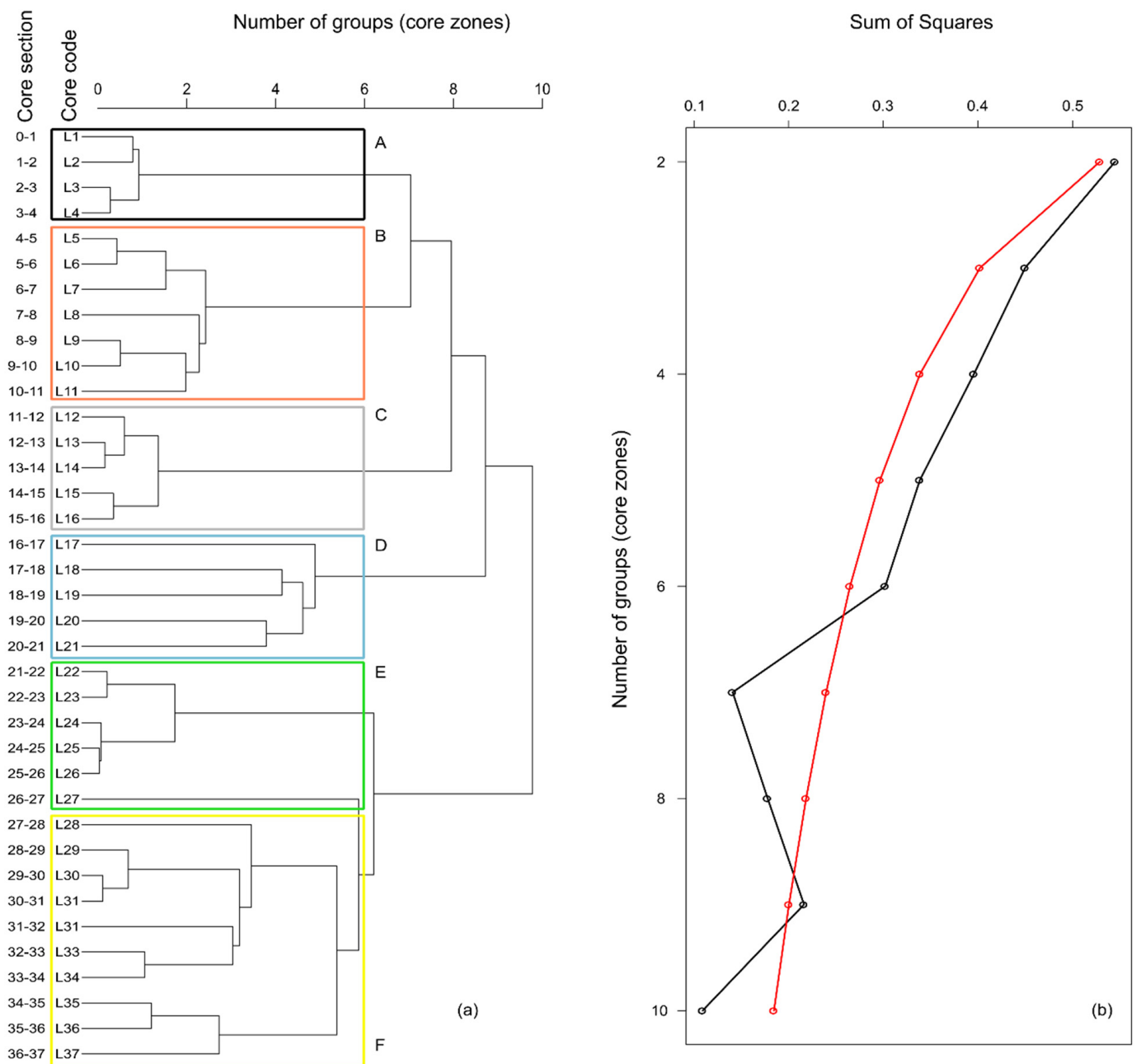


Figure 5. Cluster analysis defining stratigraphic zones (groups of sections) along the core based on the chironomid assemblages in the Upper Balma Lake (a) and broken sticks analysis defining the proper number of groups (b) ($n = 6$). Obtained stratigraphic zones are indicated with the same colors used for RDA analysis (see Figure 6a).

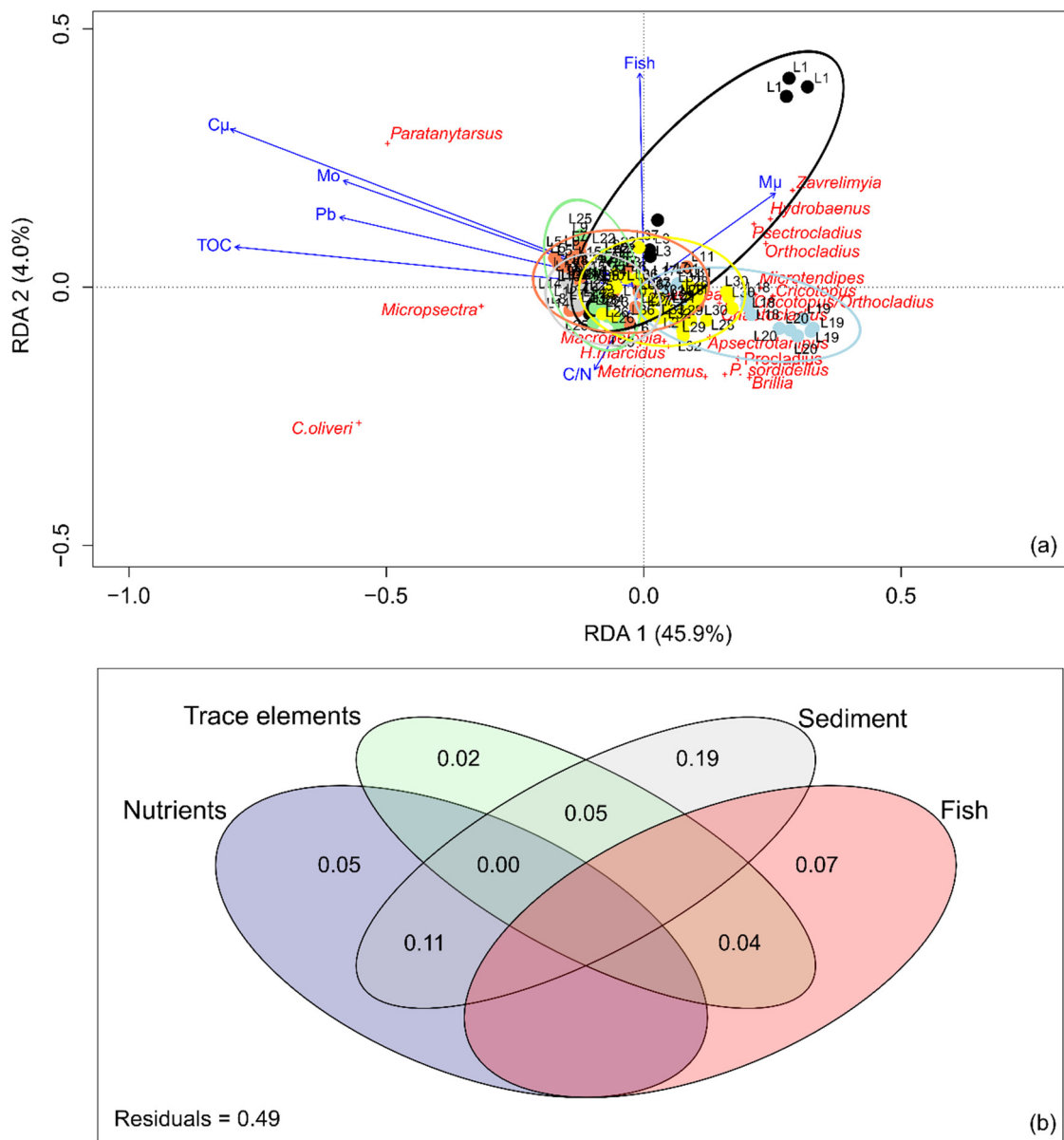


Figure 6. (a) Redundancy Analyses (RDA) illustrate the associations between chironomid taxa and the variables under consideration and (b) Venn diagrams depict the results of variance partitioning analysis (VPA) for the four variable groups: nutrients (TOC and C/N ratio), trace elements (Pb, Mo), sediment characteristics (first percentile C_{μ} and median diameter M_{μ}), and the presence of fish in relation to chironomid taxa. Variance that is unexplained or accounts for less than 1% is omitted. The group colors used in the RDA analysis correspond to those in the cluster analysis (refer to Figure 5).

3.3. Relationships Between Subfossil Assemblages and Environmental Features

A strong significant correlation was observed among percentages of sand, silt, and clay ($r > 0.90, p < 0.001$) and with C_{μ} and M_{μ} ($r > 0.66, p < 0.001$). Therefore, only C_{μ} and M_{μ} were considered representative of sediment characteristics for further analysis, as their correlation was under the threshold level ($r = -0.23, p < 0.05$). The Total Organic Carbon (TOC) was weakly correlated to C/N ratio ($r = -0.37, p < 0.05$) and highly correlated with TN ($r = 0.89, p < 0.001$). Therefore, the latter feature was excluded from the analysis. Highly significant correlations were observed among trace elements ($r \geq 0.69, p < 0.001$). Therefore, Pb was chosen as a presentative trace element, and Mo was also kept in the model, as its peaks can be related to hypoxia conditions (Boothman et al., 2022), which can affect Chironomid communities. The dataset utilized for RDA and VPA analyses comprised TOC

and C/N ratio for nutrient parameters, Pb and Mo for trace elements, and C_{μ} percentile and M_{μ} median diameter for sediment characteristics. The results of the RDA application are shown in Figure 6a.

The RDA 1 and RDA 2 axes were both significant, accounting for 45.9% and 4.0% of the observed variability, respectively (Figure 6a; Table 4). The primary gradient, represented by RDA 1, is closely linked with TOC, trace elements, and C_{μ} , while RDA 2 appears to be more associated with the presence of fish. All the variable groups considered to explain the variation in subfossil chironomid assemblages throughout the core were significant (Table 4), collectively accounting for 51.1% of the total variance (Figure 6b). Of the individual factors, sediment characteristics explained the largest portion of the variation (19.0%), with the interaction between sediment and nutrients accounting for 11.0%. Fish presence explained 7.0% of the variation, and trace elements contributed a minor portion (2.4%).

Table 4. Outcomes of (a) Redundancy Analysis (RDA) and (b) Variance Partitioning Analysis (VPA) conducted on Chironomidae taxa found in sediment core samples from Balma Lake. VPA variable groups included nutrients (TOC and C/N ratio), trace elements (Pb, Mo), sediment properties (first percentile C_{μ} and median diameter M_{μ}), and fish presence.

(a) RDA					
	RDA1	RDA2	RDA3		
Eigenvalue	0.014	0.001	0.001		
Proportion Explained	0.459	0.040	0.022		
Cumulative Proportion	0.459	0.499	0.521		
Significance (999 permutations)	0.001	0.003	0.049		
(b) VPA					
Variable	Adjusted r^2	d.f.	F	p -Level	
Sediment + Nutrients + trace elements + Fish	0.511	7	17.437	<0.001	
Sediment	0.333	2	28.505	<0.001	
Nutrients	0.319	2	26.777	<0.001	
Trace elements	0.178	2	12.935	<0.001	
Fish	0.018	1	3.047	0.045	

4. Discussion

Lacustrine sediments provide a continuous chronological record that reveals the historical conditions of a lake [56–59]. By examining sediment layers formed in environments with varying energy levels, researchers can reconstruct periods of alluvial activity influenced by climatic patterns, particularly rainfall and extreme weather events [10,11,29]. The thickness of these alluvial layers serves as an indicator of the intensity of such events [12,13]. This study focused on analyzing chironomid communities in an alpine lake, considering factors such as nutrient levels, trace elements, sediment properties, and the presence of fish.

4.1. Sediment Core Characteristics and Flood Events in Alpine Areas

From a sedimentological perspective, the examined core revealed various distinct zones, with an intense alternation of coarse and fine sediments at the bottom, a noticeable but reduced alternation in the central section, and massive sediments at the top. These structures seem to correspond to fluctuations in rainfall patterns, with peaks in coarse sediments within the grain size distribution of the core indicating intense or extreme weather events. The observed sediment textures suggest that heavy rainfall periods are associated with core sections at depths between 8 and 12 cm (L8–L12), 17 and 22 cm (L17–L22), and 28 and 32 cm (L28–L32). These observations are consistent with findings from other high-altitude alpine lakes as reported by several researchers [60,61]. In alpine lakes, sediment deposition dynamics are closely linked to the characteristics of the lake's drainage area. Large catchment areas composed of easily erodible materials, such as periglacial deposits, contribute

to higher sedimentation rates through processes like glacier erosion, frost-induced rock breakage, overgrazing, or heavy rainfall [10]. Additional deposition processes may include wind erosion, bank erosion due to ice or wave action, and direct contributions from glacial sediments [62]. Coarse grain sizes in sediment records serve as indicators of flood intensity in lake catchments [63,64], and examining sediment archives can help estimate changes in flood and rainfall periods. For example, Moreno et al. [11] reconstructed intense rainfall events during the Little Ice Age (LIA) compared to the Medieval Warm Period (MWP) in a Spanish alpine lake. In the Italian Alps, the distribution of debris-flow layers over the past 2000 years has been interpreted as evidence of frequent extreme rainfall events [13]. As sediment characteristics are crucial for macrobenthic invertebrate communities in freshwater environments, these changes can significantly influence the structure of chironomid assemblages over centuries, alongside other environmental and climatic factors.

4.2. Geochemistry in Core Layers

An additional method for reconstructing past environmental conditions through paleolimnological analyses involves examining the organic matter (OM) content in sediment layers. The primary sources of OM include aquatic organisms and contributions from the surrounding shorelines and terrestrial areas. Peaks in total nitrogen (TN) and total organic carbon (TOC) within the sediment core are likely linked to warmer periods, increased solar radiation, and higher pH levels, which enhance lake productivity. The C/N molar ratio is frequently employed to qualitatively differentiate the contributions of terrestrial vegetation and aquatic organisms to the organic carbon in lake sediments. Typically, terrestrial vascular plants have low nitrogen content, resulting in high C/N ratios, while aquatic plants have higher nitrogen content and lower C/N ratios [65,66]. It is suggested that phytoplankton have a C/N ratio of less than 10 [67]. A C/N ratio exceeding 20 indicates a significant terrestrial OM input, whereas values between 10 and 20 suggest a mix of aquatic and terrestrial plant contributions [68–70].

In the Upper Balma core, C/N ratios ranged from 9.9 to 36.4, generally indicating high levels and suggesting a combination of aquatic and terrestrial plant presence [71]. Ratios above 20 point to a predominance of terrestrial OM. Notably, at specific core depths (10, 26, and 30 cm), values surpass 30, signaling substantial terrestrial material input likely associated with intense flooding and heavy rainfall events. Conversely, depths of 19 and 34 cm highlight a predominance of lake-derived OM, indicative of climatic periods with reduced rainfall and diminished terrestrial OM input. Trace elements along the sediment core showed concentration patterns consistent with other lake ecosystem studies. Lead (Pb) levels in sediments are primarily attributed to atmospheric pollution, which began during the Roman Empire and surged after the Industrial Revolution (around 1850), peaking in the 1970s due to the use of leaded fuels [72,73]. Similar peaks of Pb levels in core sediments of the lacustrine ecosystem were widely recorded in many studies [10,27,28,31,32,47,57] allowing us to associate the core sections showing these peaks to a period corresponding to the 1970s decade, when fish were introduced in the Piedmont area alpine lakes [6]. This trend reversed following the introduction of strict emission controls and lead-free fuels [27,28,74]. Similar trends were observed for zinc (Zn) and cadmium (Cd), with concentrations decreasing from the top to the bottom of the core and highest levels in recent layers [57]. Elevated molybdenum (Mo) concentrations in sediments may indicate anoxic events, impacting the chironomid community [75].

4.3. Subfossil Chironomid Assemblages

The analyzed assemblages were predominantly composed of typical alpine taxa. The genus *Paratanytarsus* was the most prevalent, found in every section, and is commonly one of the most frequent and often dominant midges in alpine [18–77]. Significant abundances were also noted for *Micropsectra* and *Corynocera oliveri* (present in 36 sections), which are cold stenothermic insects usually associated with oligotrophic environments [15]. Additionally, another alpine species indicative of oligotrophic conditions, *Heterotrissocladius marcidus*,

was widely present in many sections analyzed ($n = 20$). The subfamily Orthocladiinae was well represented throughout the core profile and includes species adapted to low water temperatures and the harsh conditions of high-altitude environments [18,76,78]. The prevalence of Tanytarsini, the widespread occurrence of *H. marcidus*, the numerous genera belonging to the Orthocladiinae, and the absence of Chironomini (except in the topmost section) are generally linked to stable oligotrophic conditions [6]. This indicates that despite observed variations in the core profile, Upper Balma Lake has remained relatively oligotrophic over the past 1200 years. These findings are consistent with paleolimnological studies conducted in Lower Balma Lake [6], which is hydrologically connected to the Upper Lake by a small creek. While the subfossil communities in the Upper Lake indicate general oligotrophic conditions, biodiversity showed notable fluctuations along the sediment core, associated with changes in the abundance of certain taxa, as evidenced by ANOSIM and SIMPER tests. Intense rainfall regimes can reduce biodiversity [79], aligning with trends in the main community indices calculated for the Upper Balma core. Variations in chironomid assemblages are likely influenced by changes in sediment texture and nutrient loads from the surrounding landscape, as highlighted by RDA and VPA analyses. This may explain the increased abundance of taxa such as *Brillia*, *Chaetocladius*, *Cricotopus*, *Psectrocladius*, *Cricotopus/Orthocladius*, and *Parorthocladius*, which are commonly associated with organic matter detritus and vegetation [6,15,76]. The high abundance of these taxa may correspond to periods of heavy rainfall. *Paratanytarsus* is also linked to aquatic vegetation and algae [15,80], which were commonly observed in the Upper Lake and increased during periods of intense rainfall (Figure 4). During these times, the frequency of *Macropelopia*, a cold stenothermic predator associated with increasing temperatures in alpine lakes due to climate change [81], also rose. This suggests a relative increase in water temperatures during periods of intense rainfall, usually associated with warmer periods [8]. The appearance of *Zavrelimyia* in surface layers indicates an adaptation to warm temperatures and shallow habitats, possibly related to increased lake productivity during hot summers and global warming [82], as observed in the Lower Lake [6]. A significant reduction in biodiversity in section L19 may be linked to gravity-reworked sediments caused by slope failure from seismic activity or extreme events [83,84]. Ongoing analysis of other biological proxies, such as diatoms and testate amoebae, will provide further insights into this point.

Lastly, chironomid assemblages appear to be partially influenced by fish presence in the top sections (L1–L5), although this impact seems less significant than factors related to climatic effects, such as sediment variations and nutrient loads from rainfall regimes. Fish introduction can dramatically affect lakes through predation and trophic web alterations [85], leading to a decrease in some predators and detritivore taxa and an increase in grazer organisms [17]. In Upper Balma Lake, grazers like *C. oliveri*, *Micropsectra*, and *H. marcidus* decreased in the top core sections corresponding to the fish introduction period, consistent with paleolimnological analyses in Lower Lake [6]. The concurrent occurrence of alien fish introduction and global warming complicates the separation of individual factors as primary drivers for changes in chironomid assemblages, with overlapping effects from climatic factors [6,17,20]. As seen in the Lower Lake, trends in Upper Balma Lake likely reflect increased water temperatures due to global warming. However, fish introduction could bias temperature reconstructions for the last century, overlapping with global warming [8,86].

5. Conclusions

This research examines the geochemical properties and subfossil chironomid communities within a sediment core extracted from an alpine lake (Upper Balma Lake) in the western Italian Alps. The goal is to understand how variations in rainfall and flood patterns over the past 1200 years have impacted the region. The findings reveal periods of community restructuring linked to changes in sediment and nutrient inputs driven by rainfall variations. This study enhances our understanding of the factors influencing alpine lake ecosystems, particularly in relation to significant flood events, an area that remains

underexplored. Further analysis of other paleo-communities, such as diatom and testate amoebae assemblages, is recommended to gain a more comprehensive understanding of system dynamics. Comparisons with studies from other lakes, like Lower Balma Lake, which exhibited both similar and differing trends due to catchment differences, underscore the importance of context-specific analyses. Given the increasing impact of global climate change on rainfall patterns and the frequency of extreme events, it is crucial to deepen our knowledge of these effects. Studying paleo-communities in alpine sediment records can offer valuable insights into these dynamics.

Author Contributions: Conceptualization, M.B., P.P., D.B. and E.P. (Elisabetta Pizzul); Data curation, M.B. and P.P.; Investigation, M.B., G.S., R.M., E.P. (Elena Pavoni), P.P., G.E., M.P. and E.P. (Elisabetta Pizzul); Methodology, G.S., R.M., E.P. (Elena Pavoni), P.P., G.E., D.B., M.P. and E.P. (Elisabetta Pizzul); Supervision, M.P. and E.P. (Elisabetta Pizzul); Visualization, P.P.; Writing—original draft, M.B. and G.S.; Writing—review and editing, M.B., E.P. (Elena Pavoni), P.P. and E.P. (Elisabetta Pizzul). All authors have read and agreed to the published version of the manuscript.

Funding: This study received partial funding from the Fondazione CRT through the ALPLA III project, grant number IZSPLV 23D02.

Institutional Review Board Statement: Not applicable.

Data Availability Statement: The original contributions presented in the study are included in the article, further inquiries can be directed to the corresponding author.

Acknowledgments: We express our gratitude to Marco Rosa Clot from GeoStudio RC (Giaveno, Italy) for supplying the tools and conducting the data processing for the bathymetric analyses.

Conflicts of Interest: The authors declare no conflicts of interest.

References

- Catalan, J.; Camarero, L.; Felip, M.; Pla, S.; Ventura, M.; Buchaca, T.; Bartumeus, F.; de Mendoza, G.; Miró, A.; Casamayor, E.; et al. High mountain lakes: Extreme habitats and witnesses of environmental changes. *Limnetica* **2006**, *25*, 551–584. [[CrossRef](#)]
- Pastorino, P.; Elia, A.C.; Pizzul, E.; Bertoli, M.; Renzi, M.; Prearo, M. The old and the new on threats to high-mountain lakes in the Alps: A comprehensive examination with future research directions. *Ecol. Indic.* **2024**, *160*, 111812. [[CrossRef](#)]
- Magnea, U.; Sciascia, R.; Paparella, F.; Tiberti, R.; Provenzale, A. A model for high-altitude alpine lake ecosystems and the effect of introduced fish. *Ecol. Model.* **2013**, *251*, 211–220. [[CrossRef](#)]
- Andersen, T.; Sæther, O.A.; Cranston, P.S.; Epler, J.H. The larvae of Orthocladiinae (Diptera: Chironomidae) of the Holarctic Region—Keys and diagnoses. *Insect Syst. Evol. Suppl.* **2013**, *66*, 189–385.
- Moser, K.A.; Baron, J.S.; Brahney, J.; Oleksy, I.A.; Saros, J.E.; Hundey, E.J.; Sadro, S.; Kopáček, J.; Sommaruga, R.; Kainz, M.J.; et al. Mountain lakes: Eyes on global environmental change. *Glob. Planet. Chang.* **2019**, *178*, 77–95. [[CrossRef](#)]
- Perilli, S.; Pastorino, P.; Bertoli, M.; Salvi, G.; Franz, F.; Prearo, M.; Pizzul, E. Changes in midge assemblages (Diptera Chironomidae) in an alpine lake from the Italian Western Alps: The role and importance of fish introduction. *Hydrobiologia* **2020**, *847*, 2393–2415. [[CrossRef](#)]
- Beniston, M.; Diaz, H.F.; Bradley, R.S. Climatic change at high elevation sites: An overview. *Clim. Chang.* **1997**, *36*, 233–251. [[CrossRef](#)]
- Giguet-Covex, C.; Arnaud, F.; Enters, D.; Poulencard, J.; Millet, L.; Francus, P.; David, F.; Rey, P.J.; Delannoy, J.J. Quaternary research at the interface of erosion, sedimentation and environmental changes in high-altitude mountain catchments. *Quat. Res.* **2012**, *77*, 12–22. [[CrossRef](#)]
- Trenberth, K.E. Conceptual framework for changes of extremes of the hydrological cycle with climate change. *Clim. Chang.* **1999**, *42*, 327–339. [[CrossRef](#)]
- Arnaud, F.; Poulencard, J.; Giguet-Covex, C.; Wilhelm, B.; Révillon, S.; Jenny, J.P.; Revel, M.; Enters, D.; Bajard, M.; Fouinat, L.; et al. Erosion under climate and human pressures: An alpine lake sediment perspective. *Quat. Sci. Rev.* **2016**, *152*, 1–18. [[CrossRef](#)]
- Moreno, A.; Valero-Garcés, B.; Gonzales-Sampériz, P.; Rico, M. Flood response to rainfall variability during the last 2000 years inferred from the Taravilla Lake record (Central Iberian Range, Spain). *J. Paleolimnol.* **2008**, *40*, 943–961. [[CrossRef](#)]
- Nesje, A.; Olaf Dahl, S.; Matthews, J.A.; Berrisdorf, M.S. A 4500 years of river floods obtained from a sediment core in Lake Atnsjoen, eastern Norway. *J. Paleolimnol.* **2001**, *25*, 329–342. [[CrossRef](#)]
- Irmler, R.; Daut, G.; Mäusbacher, R. A debris flow calendar derived from sediments of lake Lago di Braies (N. Italy). *Geomorphology* **2006**, *77*, 69–78. [[CrossRef](#)]
- Rebetz, M.; Lugon, R.; Baeriswyl, P.A. Climatic change and debris flow in high-mountain regions: The case study of the Ritigraben torrent (Swiss Alps). *Clim. Chang.* **1997**, *36*, 371–389. [[CrossRef](#)]

15. Brooks, S.J.; Langdon, P.G.; Heiri, O. *The Identification and Use of the Palearctic Chironomidae Larvae in Palaeoecology*; Quaternary Research Association: London, UK, 2007.
16. Cao, Y.; Zhang, E.; Langdon, P.G.; Liu, E.; Shen, J. Chironomid-inferred environmental change over the past 1400 years in the shallow, eutrophic Taibai Lake (southeast China): Separating impacts of climate and human activity. *Holocene* **2014**, *24*, 581–590. [[CrossRef](#)]
17. Raposeiro, P.M.; Rubio, M.J.; González, A.; Hernández, A.; Sánchez-López, G.; Vázquez-Loureiro, D.; Rull, V.; Bao, R.; Costa, A.C.; Gonçalves, V.; et al. Impact of the historical introduction of exotic fishes on the chironomid community of Lake Azul (Azores Islands). *Palaeogeogr. Palaeoclim. Palaeoecol.* **2017**, *466*, 77–88. [[CrossRef](#)]
18. Füreder, L.; Ettinger, R.; Boggero, A.; Thaler, B.; Thies, H. Macroinvertebrate diversity in Alpine lakes: Effects of altitude and catchment properties. *Hydrobiologia* **2006**, *652*, 123–144. [[CrossRef](#)]
19. Moller Pillot, H.K.M. *Chironomidae Larvae I—Biology and Ecology of the Tanytopodinae*; KNNV Publishing: Zeist, The Netherlands, 2009.
20. Williams, N.; Rieradevall, M.; Añón Suárez, D.; Rizzo, A.; Daga, R.; Ribeiro Guevara, S.; Arribére, M. Chironomids as indicators of natural and human impacts in a 700-yr record from the northern Patagonian Andes. *Quat. Res.* **2016**, *86*, 120–132. [[CrossRef](#)]
21. Bertoli, M.; Pizzul, E.; Basile, S.; Perilli, S.; Tauler, R.; Lacorte, S.; Prearo, M.; Pastorino, P. Littoral macrobenthic invertebrates of two high-altitude lakes in the Alps: A small-scale analysis. *Ecohydrol. Hydrobiol.* **2023**, *23*, 211–223. [[CrossRef](#)]
22. Pastorino, P.; Anselmi, S.; Esposito, G.; Bertoli, M.; Pizzul, E.; Barceló, D.; Elia, A.C.; Dondo, A.; Prearo, M.; Renzi, M. Microplastics in biotic and abiotic compartments of high-mountain lakes from Alps. *Ecol. Indic.* **2023**, *150*, 110215. [[CrossRef](#)]
23. Heiri, O.; Lotter, A.F.; Hausmann, S.; Kienast, F. A Chironomid-Based Holocene Summer Air Temperature Reconstruction from the Swiss Alps. *Holocene* **2003**, *13*, 477–484. [[CrossRef](#)]
24. Hedges, J.; Stern, J. Carbon and Nitrogen Determinations of Carbonate-Containing Solids. *Limnol. Oceanogr.* **1984**, *29*, 657–663. [[CrossRef](#)]
25. Heaton, T.J.; Köhler, P.; Butzin, M.; Bard, E.; Reimer, R.W.; Austin, W.E.N.; Bronk Ramsey, C.; Grootes, P.M.; Hughen, K.A.; Kromer, B.; et al. Marine20—The Marine Radiocarbon Age Calibration Curve (0–55,000 CAL BP). *Radiocarbon* **2020**, *62*, 779–820. [[CrossRef](#)]
26. Shotyk, W.; Weiss, D.; Appleby, P.G.; Cheburkin, A.K.; Gloor, R.F.M.; Kramers, J.; Reese, S.; Van Der Knaap, W.O. History of Atmospheric Lead Deposition Since 12,370 14C yr BP from a Peat Bog, Jura Mountains, Switzerland. *Science* **1998**, *281*, 1635–1640. [[CrossRef](#)]
27. Brännvall, M.L.; Bindler, R.; Emteryd, O.; Renberg, I. Four Thousand Years of Atmospheric Lead Pollution in Northern Europe: A Summary from Swedish Lake Sediments. *J. Paleolimnol.* **2001**, *25*, 421–435. [[CrossRef](#)]
28. Renberg, I.; Bindler, R.; Brännvall, L. Using the Historical Atmospheric Lead-Deposition Record as a Chronological Marker in Sediment Deposits in Europe. *Holocene* **2001**, *11*, 511–516. [[CrossRef](#)]
29. Arnaud, F.; Revel, M.; Winiarski, T.; Bosch, D.; Chapron, E.; Desmet, M.; Tribouvillard, N. Lead Fall-Out Isotopic Signal over French Northern Alps: Timing and Sources Constraints from Distant Lake Sediment Records. *J. Phys. IV Fr.* **2003**, *107*, 61–64. [[CrossRef](#)]
30. Arnaud, F.; Revel-Rolland, M.; Bosch, D.; Winiarski, T.; Desmet, M.; Tribouvillard, N.; Givilet, N. A 300-Year History of Lead Contamination in Northern French Alps Reconstructed from Distant Lake Sediment Records. *J. Environ. Monit.* **2004**, *6*, 448–456. [[CrossRef](#)]
31. Spadini, L.; Sturm, M.; Wehrli, B.; Bott, M. Analysis and Dating of Pb, Cd, Cu, Zn Sediment Profiles from the Vitznau Basin of Lake Lucerne (Switzerland). *Rev. Geogr. Alpine* **2003**, *91*, 41–48.
32. Camarero, L.; Botev, I.; Muri, G.; Psenner, R.; Rose, N.; Stuchlik, E. Trace Elements in Alpine and Arctic Lake Sediments as a Record of Diffuse Atmospheric Contamination across Europe. *Freshw. Biol.* **2009**, *54*, 2518–2532. [[CrossRef](#)]
33. Nedjai, R.; Motelica, M.; Bensaid, A.; Azaroual, A. Identification of Heavy Metal Contamination in Lake Sediments Using Lead Isotopes: The Case of Saint-Point and Grand Maclu Lakes (France). *Water Product. J.* **2021**, *1*, 75–85. [[CrossRef](#)]
34. Blaauw, M.; Christen, J.A.; Aquino Lopez, M.A.; Vazquez, J.E.; Gonzalez, O.M.V.; Belding, T.; Theiler, J.; Gough, B.; Karney, C. Rbacon: Age-Depth Modelling Using Bayesian Statistics. R Package Version 3.2.0. Available online: <https://cran.r-project.org/package=rbacon> (accessed on 4 November 2024).
35. Oliver, D.R. The Larvae of Diamesinae (Diptera: Chironomidae) of the Holarctic Region—Keys and Diagnoses. In *Chironomidae of the Holarctic Region—Keys and Diagnoses. Part 1: Larvae*; Wiederholm, T., Ed.; Entomologica Scandinavica: Supplement; 1983; Volume 19, pp. 115–138.
36. Pinder, L.C.V.; Reiss, F. The larvae of Chironominae (Diptera: Chironomidae) of the Holarctic region—Keys and diagnoses. In *Chironomidae of the Holarctic Region—Keys and Diagnoses. Part 1: Larvae*; Wiederholm, T., Ed.; Entomologica Scandinavica: Supplement; 1983; Volume 19, pp. 293–435.
37. Sæther, O.A. The larvae of Prodiamesinae (Diptera: Chironomidae) of the Holarctic region—Keys and diagnoses. In *Chironomidae of the Holarctic Region—Keys and Diagnoses. Part 1: Larvae*; Wiederholm, T., Ed.; Entomologica Scandinavica: Supplement; 1983; Volume 19, pp. 141–147.
38. Lencioni, V.; Marziali, L.; Rossaro, B. *I Ditteri Chironomidi, Morfologia, Tassonomia, Ecologia, Fisiologia e Zoogeografia*; MUSE-Museo delle Scienze: Trento, Italy, 2007.
39. Moller Pillot, H.K.M. *Chironomidae Larvae II—Biology and Ecology of the Chironomini*; KNNV Publishing: Zeist, The Netherlands, 2009.

40. Moller Pillot, H.K.M. *Chironomidae Larvae III—Biology and Ecology of the Orthoclaadiinae*; KNNV Publishing: Zeist, The Netherlands, 2009.
41. Clarke, K.R.; Somerfield, P.J.; Chapman, M.G. On resemblance measures for ecological studies, including taxonomic dissimilarities and a zero-adjusted Bray-Curtis coefficient for denuded assemblages. *J. Exp. Mar. Biol. Ecol.* **2006**, *330*, 55–80. [[CrossRef](#)]
42. Grimm, E.C. CONISS: A FORTRAN 77 program for stratigraphically constrained cluster analysis by the method of incremental sum of squares. *Comput. Geosci.* **1987**, *13*, 13–35. [[CrossRef](#)]
43. Bennett, K. Determination of the number of zones in a biostratigraphic sequence. *New Phytol.* **1996**, *132*, 155–170. [[CrossRef](#)]
44. Rigterink, S.; Echeverría-Galindo, P.; Martínez-Abarca, R.; Massaferró, J.; Hoelzmann, P.; Wünnemann, B.; Laug, A.; Pérez, L.; Kang, W.; Börner, N.; et al. Subfossil chironomids as indicators of hydrological changes in the shallow and high-altitude lake Shen Co, Tibetan Plateau, over the past two centuries. *J. Limnol.* **2022**, *81*, 2077. [[CrossRef](#)]
45. Juggins, S. Rioja: Analysis of Quaternary Science Data, R Package Version 0.9-15.1. 2017. Available online: <https://cran.r-project.org/package=rioja> (accessed on 4 November 2024).
46. Clarke, K.R. Non-parametric multivariate analyses of changes in community structure. *Austral Ecol.* **1993**, *18*, 117–143. [[CrossRef](#)]
47. Anderson, M.J. Distance-based tests for homogeneity of multivariate dispersions. *Biometrics* **2006**, *62*, 245–253. [[CrossRef](#)]
48. Legendre, P.; Legendre, L.F.J. *Numerical Ecology*; Elsevier Science: Amsterdam, The Netherlands, 1998.
49. ter Braak, C.J.F.; Šmilauer, P. *CANOCO Release 4. Reference Manual and Users Guide to CANOCO for Windows: Software for Canonical Community Ordination*; Microcomputer Power: Ithaca, NY, USA, 1998.
50. ter Braak, C.J.F.; Šmilauer, P. *CANOCO Reference Manual and User's Guide: Software for Ordination (Version 5.0)*; Microcomputer Power: Ithaca, NY, USA, 2012.
51. Dormann, C.F.; Elith, J.; Bacher, S.; Buchmann, C.; Gudrun, C.; Carré, G.; Marquéz, J.R.G.; Gruber, B.; Lafourcade, B.; Leitão, P.J.; et al. Collinearity: A review of methods to deal with it and a simulation study evaluating their performance. *Ecography* **2013**, *36*, 27–46. [[CrossRef](#)]
52. Borcard, D.P.; Legendre, P.; Drapeau, P. Partialling out the spatial component of ecological variation. *Ecology* **1992**, *73*, 1045–1055. [[CrossRef](#)]
53. R Core Team. *R: A Language and Environment for Statistical Computing*; R Foundation for Statistical Computing: Vienna, Austria, 2021. Available online: <https://www.R-project.org/> (accessed on 4 November 2024).
54. R Studio Team. *RStudio. Integrated Development Environment for R*; R Studio, PBC: Boston, MA, USA, 2021. Available online: <http://www.rstudio.com/> (accessed on 4 November 2024).
55. Wilhelm, B.; Arnaud, F.; Sabatier, P.; Crouzet, C.; Brisset, E.; Chaumillon, E.; Disnar, J.R.; Guitier, F.; Malet, E.; Reyss, J.L.; et al. 1400 years of extreme precipitation patterns over the Mediterranean French Alps and possible forcing mechanisms. *Quat. Res.* **2012**, *78*, 1–12. [[CrossRef](#)]
56. Cantonati, M.; Zorza, R.; Bertoli, M.; Pastorino, P.; Salvi, G.; Platania, G.; Prearo, M.; Pizzul, E. Recent and subfossil diatom assemblages as indicators of environmental change (including fish introduction) in a high-mountain lake. *Ecol. Indic.* **2021**, *125*, 107603. [[CrossRef](#)]
57. Salvi, G.; Bertoli, M.; Giubileo, C.; Pastorino, P.; Pavoni, E.; Crosera, M.; Prearo, M.; Pizzul, E. Testate Amoeba and Chironomid assemblages from Balma Lake (Piedmont, Italy): A multi-proxy record to identifying recent climate and environmental changes in alpine areas. *Quat. Sci. Rev.* **2022**, *285*, 107547. [[CrossRef](#)]
58. Nedjai, R.; Nguyen-Trung, C.; Messaoud-Nacer, N. Multi-Secular Lead (Pb) Contamination on a Regional Scale: Comparative Analysis of the Grand-Maclu and Saint-Point Lakes in the Jura Area, France. *J. Adv. Chem. Eng.* **2011**, *1*, 1–10. [[CrossRef](#)]
59. Schillereff, D.N.; Chiverrell, R.C.; Macdonald, N.; Hooke, J.M. Flood stratigraphies in lake sediments: A review. *Earth-Sci. Rev.* **2004**, *135*, 17–37. [[CrossRef](#)]
60. Wilhelm, B.; Arnaud, F.; Sabatier, P.; Magand, O.; Chapron, E.; Courp, T.; Tachikawa, K.; Fanget, B.; Malet, E.; Pignol, C.; et al. Palaeoflood activity and climate change over the last 1400 years recorded by lake sediments in the north-west European Alps. *J. Quat. Sci.* **2013**, *28*, 189–199. [[CrossRef](#)]
61. Fouinat, L.; Sabatier, P.; Poulenard, J.; Etienne, D.; Crouzet, C.; Develle, A.L.; Doyen, E.; Malet, E.; Reyss, J.L.; Sagot, C.; et al. One thousand seven hundred years of interaction between glacial activity and flood frequency in proglacial Lake Muzelle (western French Alps). *Quat. Res.* **2017**, *87*, 407–422. [[CrossRef](#)]
62. Rubensdotter, L.; Rosqvist, G. Influence of geomorphological setting, fluvial-, glaciofluvial- and mass-movement processes on sedimentation in alpine lakes. *Holocene* **2009**, *19*, 665–678. [[CrossRef](#)]
63. Beierle, B.D.; Lamoureux, S.F.; Cockburn, J.M.H.; Spooner, I. A new method for visualizing sediment particle size distributions. *J. Paleolimnol.* **2002**, *27*, 279–283. [[CrossRef](#)]
64. Francus, P.; Bradley, R.S.; Abbott, M.B.; Patridge, W.; Keimig, F. Paleoclimate studies of minerogenic sediments using annually resolved textural parameters. *Geophys. Res. Lett.* **2002**, *29*, 1998. [[CrossRef](#)]
65. Meyers, P.A.; Lallier-Vergès, E. Lacustrine Sedimentary Organic Matter Records of Late Quaternary Paleoclimates. *J. Paleolimnol.* **1998**, *21*, 345–372. [[CrossRef](#)]
66. Müller, A.; Mathesius, U. The Palaeoenvironments of Coastal Lagoons in the Southern Baltic Sea, I. The Application of Sedimentary Corg/N Ratios as Source Indicators of Organic Matter. *Palaeogeogr. Palaeoclimatol. Palaeoecol.* **1999**, *145*, 1–16. [[CrossRef](#)]
67. Hedges, J.I.; Oades, J.M. Comparative Organic Geochemistries of Soils and Marine Sediments. *Org. Geochem.* **1997**, *27*, 319–361. [[CrossRef](#)]

68. Talbot, M.R.; Johannessen, T. A High Resolution Palaeoclimatic Record for the Last 27,500 Years in Tropical West Africa from the Carbon and Nitrogen Isotopic Composition of Lacustrine Organic Matter. *Earth Planet. Sci. Lett.* **1992**, *110*, 23–37. [[CrossRef](#)]
69. Tyson, R.V. *Sedimentary Organic Matter*; Springer: Heidelberg, Germany, 1995. [[CrossRef](#)]
70. Talbot, M.R.; Lærdal, T. The Late Pleistocene—Holocene Palaeolimnology of Lake Victoria, East Africa, Based upon Elemental and Isotopic Analyses of Sedimentary Organic Matter. *J. Paleolimnol.* **2000**, *23*, 141–164. [[CrossRef](#)]
71. Chen, X.; Meng, X.; Song, Y.; Zhang, B.; Wan, Z.; Zhou, B.; Zhang, E. Spatial Patterns of Organic and Inorganic Carbon in Lake Qinghai Surficial Sediments and Carbon Burial Estimation. *Front. Earth Sci.* **2021**, *9*, 714936. [[CrossRef](#)]
72. Thevenon, F.; Graham, N.D.; Chiaradia, M.; Arpagaus, P.; Wildi, W.; Poté, J. Local to regional scale industrial heavy metal pollution recorded in sediments of large freshwater lakes in central Europe (lakes Geneva and Lucerne) over the last centuries. *Sci. Total Environ.* **2011**, *412–413*, 239–247. [[CrossRef](#)]
73. Elbaz-Poulichet, F.; Dezileau, L.; Freyrier, R.; Cossa, D.; Sabatier, P. A 3500-Year Record of Hg and Pb Contamination in a Mediterranean Sedimentary Archive (The Pierre Blanche Lagoon, France). *Environ. Sci. Technol.* **2011**, *45*, 8642–8647. [[CrossRef](#)]
74. Siver, P.A.; Wozniak, J.A. Lead analysis of sediment cores from seven Connecticut lakes. *J. Paleolimnol.* **2001**, *26*, 1–10. [[CrossRef](#)]
75. Boothman, W.S.; Coiro, L.; Moran, S.B. Molybdenum accumulation in sediments: A quantitative indicator of hypoxic water conditions in Narragansett Bay, RI. *Estuar. Coast. Shelf Sci.* **2022**, *267*, 107778. [[CrossRef](#)]
76. Boggero, A.; Füreder, L.; Lencioni, V.; Simcic, T.; Thaler, B.; Ferrarese, U.; Ettinger, R. Littoral Chironomid Communities of Alpine Lakes in Relation to Environmental Factors. *Hydrobiologia* **2006**, *562*, 145–165. [[CrossRef](#)]
77. Hamerlík, L.; Svitok, M.; Novikmec, M.; Veselská, M.; Bitušík, P. Weak altitudinal pattern of overall chironomid richness is a result of contrasting trends of subfamilies in high-altitude ponds. *Hydrobiologia* **2017**, *793*, 67–81. [[CrossRef](#)]
78. Bretschko, G. The chironomid fauna of a high mountain lake (Vorderer Finstertaler See, Tyrol, Austria). *Entomol. Tidskrift* **1974**, *95*, 22–33.
79. Marchetto, A.; Mosello, R.; Psenner, R.; Bendetta, G.; Boggero, A.; Tait, D.; Tartari, G. Factors affecting water chemistry of alpine lakes. *Aquat. Sci.* **1995**, *57*, 81–89. [[CrossRef](#)]
80. Brodersen, K.P.; Anderson, N.J. Distribution of chironomids (Diptera) in low arctic West Greenland lakes: Trophic conditions, temperature, and environmental reconstruction. *Freshw. Biol.* **2002**, *47*, 1137–1157. [[CrossRef](#)]
81. Slobodníková, V.; Hamerlík, L.; Wojewódka-Przybył, M.; Sochuliaková, L.; Szarłowicz, K.; Buczkó, K.; Bitušík, P. Tracking fish introduction in a mountain lake over the last 200 years using chironomids, diatoms, and cladoceran remains. *Water* **2023**, *15*, 1372. [[CrossRef](#)]
82. Ilyashuk, E.A.; Koinig, K.A.; Heiri, O.; Ilyashuk, B.P.; Psenner, R. Holocene temperature variations at a high-altitude site in the Eastern Alps: A chironomid record from Schwarzsee ob Sölden, Austria. *Quat. Sci. Rev.* **2011**, *30*, 176–191. [[CrossRef](#)]
83. Arnaud, F.; Lignier, V.; Revel, M.; Desmet, M.; Pourchet, M.; Beck, C.; Charlet, F.; Trentesaux, A.; Tribouvillard, N. Flood and earthquake disturbance of 210Pb geochronology (Lake Anterne, North French Alps). *Terra Nova* **2002**, *14*, 225–232. [[CrossRef](#)]
84. Beck, C. Late Quaternary lacustrine paleo-seismic archives in north-western Alps: Examples of earthquake-origin assessment of sedimentary disturbances. *Earth-Sci. Rev.* **2009**, *96*, 327–344. [[CrossRef](#)]
85. Tiberti, R.; Von Hardenberg, A.; Bogliani, G. Ecological impact of introduced fish in high altitude lakes: A case of study from the European Alps. *Hydrobiologia* **2014**, *724*, 1–19. [[CrossRef](#)]
86. Millet, L.; Massa, C.; Bichet, V.; Frossard, V.; Belle, S.; Gauthier, E. Anthropogenic versus climatic control in a high-resolution 1500-year chironomid stratigraphy from a southwestern Greenland lake. *Quat. Res.* **2014**, *81*, 193. [[CrossRef](#)]

Disclaimer/Publisher’s Note: The statements, opinions and data contained in all publications are solely those of the individual author(s) and contributor(s) and not of MDPI and/or the editor(s). MDPI and/or the editor(s) disclaim responsibility for any injury to people or property resulting from any ideas, methods, instructions or products referred to in the content.